EXPERIMENTAL OPTIMIZATION OF TRIBOLOGICAL PROPERTIES OF ALUMINUM BRONZE ALLOYS MADE BY THE FORGING METHOD

by

Idris CESUR[a*], Aslan COBAN[a], Sefa BACAK[b], Ibrahim OZSERT[a], Omer SECGIN[a], and Akin Oguz KAPTI[c]

[a] Department of Mechanical Engineering, Faculty of Technology,
Sakarya University of Applied Sciences, Sakarya, Turkey
[b] Graduate Education Institute, Sakarya University of Applied Sciences, Sakarya, Turkey
[c] Department of Mechanical Engineering, Faculty of Engineering,
Sakarya University, Sakarya, Turkey

Original scientific paper
https://doi.org/10.2298/TSCI2304101C

Aluminum bronze alloys produced by various methods are preferred materials in many fields of the industry due to their high wear resistance and good sliding properties. This study investigated the tribological properties of aluminum bronze alloys produced by forging from Cu, Al, Fe, and Mg elements. Dry sliding wear tests were carried out on a pin-on-disc wear device. Three tribological properties, wear, friction coefficient, and temperature of aluminum bronze alloys were investigated. Experimental studies were carried out for different loads, sliding speeds, and sliding ways. The factorial experiment design method was applied in the MINITAB program. A SEM visualized the samples microstructures to examine the material wear characteristics. As a result of the study, it was determined that the applied load, sliding speed, and sliding way were effective parameters on the amount of wear and friction coefficient. The maximum amount of wear was 0.352 mg at 100 N load, 3 m/s sliding speed, and 3000 m sliding way conditions. The maximum temperature between materials under these conditions is 299 °C. The minimum amount of wear was obtained when 25 N load, 1 m/s sliding speed, and 1000 m sliding way were applied.

Key words: *aluminum bronze alloys, friction, wear, optimization*

Introduction

Aluminum bronze alloys are one of the most widely used materials in many fields of industry [1]. These materials are preferred because of their high hardness, resistance to abrasion and corrosion, and ability to withstand high temperatures [2]. Due to these features, they are used in many areas, such as bearings, water pump elements, oil pipeline valves, and heat exchangers in the industry [3, 4]. Aluminum bronze alloys are copper-based alloys containing 5-11% Al by weight and small amounts of Fe, Ni, Sn, Mn, and Si elements [5, 6]. New alloys with desired properties are obtained by adding different materials. The Fe and Ni elements in the alloy reduce grain size and improve mechanical properties [7, 8]. In addition, other elements such as Mn and Si, up to 1% by weight, improve the toughness, corrosion, and machin-

* Corresponding author, e-mail: icesur@subu.edu.tr

ing properties [6]. The aluminum content in the alloy improves the mechanical strength and yield stress [9, 10].

Wear caused by different ambient and working conditions causes significant damage on the surface over time [11]. In addition, working conditions that do not harm the surface roughness should be determined [12, 13]. For this reason, wear and friction are subjects that have been studied extensively by many researchers. The primary purpose of the studies carried out to reduce the amount of friction, and wear is to extend the life of the material [14].

Liu *et al.* [15] investigated the aluminum bronze alloy's strength, hardness, ductility, and friction-wear behavior by forging and aging. It was shown that the material strength, hardness, and friction coefficient values decreased due to the forging process. Kucita *et al.* [16] investigated the effects of coating Cu-Al-Fe aluminum bronze alloys with plasma transferred arc method on wear behavior and microstructure. As a result of the study, reductions in the coefficient of friction were determined under dry friction conditions with the coating. In addition, for a 34% dilution, the wear ratio decreases with increasing Fe content. Gamon and Aniolek [17] investigated the effects of aluminum bronze alloys ($CuAl_9Fe_3$) and manganese bronze alloys ($CuMn_{11}Al_8Fe_3Ni_3$) coating on S355J2 steel on friction and wear. According to the results, they found that aluminum bronze alloys have higher wear resistance than manganese alloys. The amount of wear in the material coated with aluminum bronze decreased by 89.36% compared to the uncoated material. Kirubakaran *et al.* [18] investigated the effects of aluminum composites containing 9% TiC and 2% MoS_2 on friction and wear using the Taguchi experimental design method. They examined the impact of load variation, sliding speed, and sliding way parameters on wear in the experimental study. As a result of the study, it was determined that the load and the sliding speed are effective parameters of the wear mechanism. Gurav *et al.* [19] experimentally investigated nickel aluminum bronze alloy friction and wear characteristics. The interaction according to the load and shear rate was analyzed as a full factorial with the experimental design. The samples were examined with a scanning electron microscope. As a result of the research, they obtained the lowest friction coefficient at the lowest load of 10N. Thapliyal and Dwivedi [20] experimentally analyzed the effects of load, sliding speed, and surface temperature on dry sliding wear of C95500 nickel aluminum bronze alloy. They performed the experiments on a pin-on-disc wear device and used a full factorial experimental design. They studied the wear mechanisms by SEM analysis. They found that sliding speed, load, and temperature were effective parameters on wear behavior. Simsek *et al.* [21] experimentally investigated the effects of adding different amounts of iron to Ni-Al bronze alloys on microstructure, hardness, and wear behavior. They added Fe (3.5%, 4%, 4.5%, and 5% by weight) to the $Cu_{10}Al_5Ni$ alloy and then subjected it to several treatments. They performed the wear tests at three different loads, four different sliding ways, and a sliding speed of 0.2 m/s. As a result of the experimental study, it was determined that the alloy containing 5% Fe had the lowest weight loss and wear rate. The amount of wear increased as the sliding way and applied load increased.

In the literature, many studies examine the tribological properties of aluminum bronze alloys, their characteristics under different conditions, and various coating methods. The microstructure and wear resistance of aluminum bronze alloys are complex, and their structure changes depending on the processes applied during production. Tribological properties are essential in determining the behavior of aluminum bronze alloys under different operating conditions. This study investigated the tribological properties of CuAlFeMn aluminum bronze alloy (Al 10%, Fe 2.5%, Mn 1%, Cu 85.5%, other 1%) widely used in the industry. The experiments were carried out in a wear measurement device operating on the pin-on-disc principle and at different loads, sliding speeds, and sliding ways.

Material and methods

The tribological properties of aluminum bronze alloy produced by the forging method were investigated. Wear and friction tests were carried out following ASTM G99 standards. The experiments were carried out on a pin-on-disc type wear device. The wear device contacts an aluminum bronze alloy fixed on an arm with an abrasive AISI 8620 cement steel disc. The schematic view of the pin-on-disc wear device is given in fig. 1.

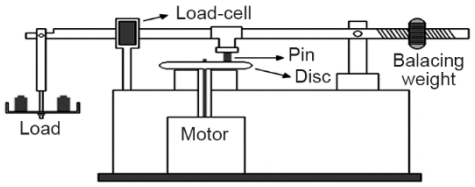

Figure 1. The schematic view of the pin-on-disc wear device

The mechanical properties of the aluminum bronze alloy used in the experiments are given in tab. 1. The test specimens were precision machined in 10 × 20 mm dimensions to be suitable for use in the wear device. In addition, 3 mm diameter holes were drilled in the samples to examine the instantaneous temperature changes during the study.

Table 1. The mechanical properties of the aluminum bronze alloy

Material	Aluminum bronze alloy	Cement steel
Norm	$CuAl_{10}Fe$	AISI8620
Tensile strength [Nmm^{-2}]	500-650	530
Yield strength [Nmm^{-2}]	180-280	385
Compression strength [Nmm^{-2}]	980-1050	980-1050
Elongation [%]	13-20	19-21
Hardness, HB	115-135	169
Specific mass [kgm^{-3}]	7.7	7.8
Al, Fe, Mn, Cu, other [%]	10, 2.5, 1, 85.5, 1	

Hardened AISI8620 cement steel was used as the abrasive disc material. Surface hardness was increased by applying the carburetion process to the abrasive disc, whose mechanical properties are given in tab. 1. The abrasive disc is heated to 850-900 ºC austenite temperature during carburation. The tempering process is performed to obtain a surface hardness of 61 HRC on the surface and a soft structure in the interior. Before the experimental study, sanding was applied to the abrasive disc and samples using 200, 600, 1200, and 2000 grit sandpapers. It was ensured that the surface roughness of the abrasive discs and samples were 0.65 and 0.70, respectively. The TR110 surface roughness device was used in the measurements. Measurements were made from a load cell mounted on the loading arm to determine the friction coefficient between the abrasive disc and aluminum bronze. A C3 series load cell with a capacity of 15 kg and a sensitivity of 1 g was used. The friction force was determined by transferring the data received from the load cell via an AD4406 indicator to the computer. The lateral loads expressed as friction force are divided by the average applied load, and the friction coefficient of the material pair is calculated.

Each test sample was weighed on a precision balance with 0.1 mg sensitivity before and after the test. The amount of wear was determined by taking the difference. The test samples were thoroughly cleaned with alcohol and dried before and after the test. A PT100 ther-

mocouple was connected to the sample to measure the temperature changes between the abrasive disc and aluminum bronze. A PID temperature controller was used to measure the temperature value. Tribological tests were carried out under 25 N, 50 N, 75 N, and 100 N loads, at sliding speeds of 1 m/s, 2 m/s, and 3 m/s, for 1000 m, 2000 m, and 3000 m sliding ways, under dry sliding conditions and at room temperature.

After the experiments were carried out, the internal structure of the samples was examined by a scanning electron microscope to inspect the damage that occurred on the aluminum bronze samples, and elementary analyzes was made.

Factorial experimental design involves exploring the impact of multiple parameters and their respective levels on the experimental material. It consists of all possible combinations that match all levels of each factor in the experiments with all levels of other factors. The factorial experimental design was made in the MINITAB program. The material wear, friction coefficient, and temperature values were analyzed in the factorial experiments under load, sliding speed, and sliding way conditions. These analyses investigated the tribological properties of aluminum bronze alloys according to the L36 series and wear parameters on AISI8620 cement steel. The test parameters and levels used in the study are given in tab. 2.

Table 2. Test parameters and levels

Test parameters	Levels			
	1	2	3	4
Load [N]	25	50	75	100
Sliding speed [ms^{-1}]	1	2	3	
Sliding way [m]	1000	2000	3000	

Results and discussion

Wear

This study investigated the wear characteristics of forged aluminum bronze alloys under various loads, sliding speeds, and sliding ways. The tests were carried out under dry sliding conditions. Figure 2 shows the interactions in wear amount for four loads (25 N, 50 N, 75 N, and 100 N), three sliding speeds (1 m/s, 2 m/s, and 3 m/s), and three sliding ways (1000 m, 2000 m, and 3000 m). When the interactions on the wear parameter were examined, it was seen that there was an increase in the amount of wear as the sliding way increased depending on the load. The minimum wear was determined in the case of a 25 N load, and 1000 m sliding way, and the maximum wear was selected in the case of 100 N load and 3000 m sliding way.

When the effects of sliding speed on wear depending on the load are examined, it is seen that the wear increases when the sliding speed increases at a constant load. In addition, wear increases with increasing load and sliding speed. The least amount of wear was obtained in the case of a 25 N load and 1 m/s sliding speed, and the highest amount of wear was obtained in the case of 100 N load and 3 m/s sliding speed.

When the effects of the sliding way on wear are examined depending on the sliding speed, it is seen that the wear increases when both the sliding way and the sliding speed increase. The least amount of wear was obtained at 1000 m sliding way and 1 m/s sliding speed, while the highest amount of wear was determined at 3000 m sliding way and 3 m/s sliding speed. The obtained results agree with the literature.

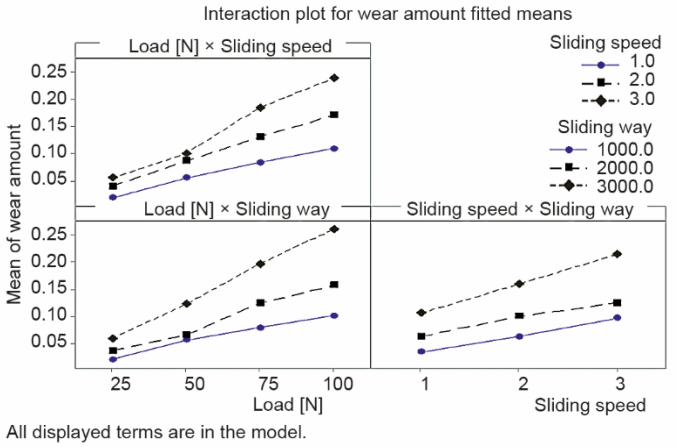

Figure 2. Wear amount interaction graph for different load, sliding speed, and sliding way conditions

Figure 3 shows the average, minimum, maximum, and optimum wear amounts for different loads, sliding speeds, and sliding ways. All test parameters considered in the experimental study are effective on wear. When the averages on the wear are examined, it is seen that the amount of wear increases as the sliding way increases. The minimum amount of wear was determined on the 1000 m sliding way, and the maximum amount was determined on the 3000 m sliding way.

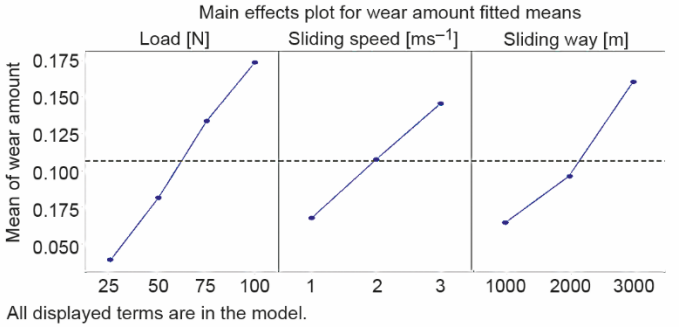

Figure 3. Average wear graph for different loads, sliding speeds, and sliding directions

Another parameter that affects the amount of wear is the applied load. The wear amount increases as the load applied to the material increases. The slightest wear was under 25 N load, and the maximum was under 100 N. The last parameter that affects the amount of wear is the sliding speed. As the sliding speed increases, the amount of wear also increases. The least amount of wear was obtained at the sliding speed of 1 m/s, and the maximum amount of wear was received at the sliding speed of 3 m/s. The optimum conditions for wear are 25 N load, 1 m/s sliding speed, and 1000 m sliding way condition. The amount of wear occurring under these conditions was determined as 0.006 mg.

Friction coefficient

Figure 4 shows the friction coefficients according to the load, sliding speed, and sliding way. When the figure is examined, it is seen that the friction coefficient increases depending on the load and the sliding speed. At the conditions of 25 N, 50 N, 75 N, and 100 N loads and 1000 m sliding way, the friction coefficients were measured as 0.25, 0.26, 0.27, and

0.30 for 1 m/s sliding speed; 0.27, 0.31, 0.35, and 0.38 for 2 m/s sliding speed; and 0.35, 0.39, 0.41, and 0.45 for 3 m/s sliding speed, respectively.

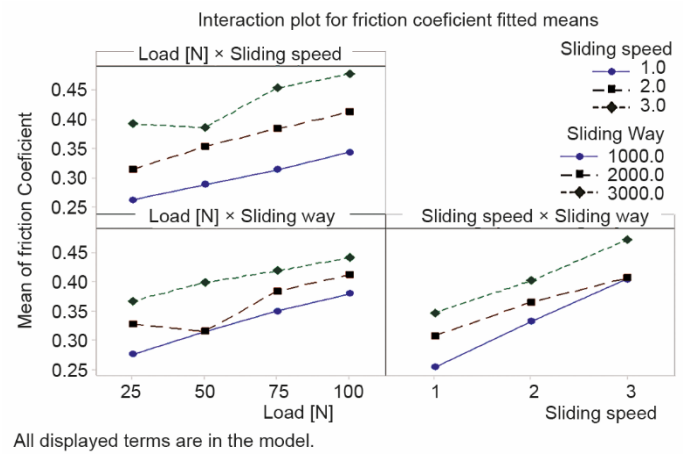

Figure 4. Friction coefficient interaction graph for different loads, sliding speeds, and sliding ways

When the results are examined, it is seen that the minimum friction coefficient is obtained in the case of 25 N load, 1 m/s sliding speed, and 1000 m sliding way, while the maximum friction coefficient is determined in the case of 100 N load, 3 m/s sliding speed and 3000 m sliding way. The friction coefficient increases with both the sliding speed and the sliding way.

Figure 5 shows the average, minimum, maximum, and optimum coefficient of friction values for various loads, sliding speeds, and sliding ways. When the graph is examined, it is seen that load, sliding speed, and sliding way are the effective parameters of the friction coefficient. The friction coefficient increases as the applied load, sliding speed, and sliding way increase. The lowest friction coefficient was determined in the case of the 1000 m sliding way, and the highest friction coefficient in the case of the 3000 m sliding way. According to the applied load, the lowest friction coefficient was obtained at 25 N load and the highest at 100 N load cases. When the effect of sliding speed on the friction coefficient is examined, the lowest friction coefficient was obtained at 1 m/s sliding speed, and the highest friction coefficient was obtained at 3 m/s sliding speed. The optimum conditions for the friction coefficient are 25 N load, 1 m/s sliding speed, and 1000 m sliding way. The average friction coefficient for these optimum conditions was determined as 0.1962.

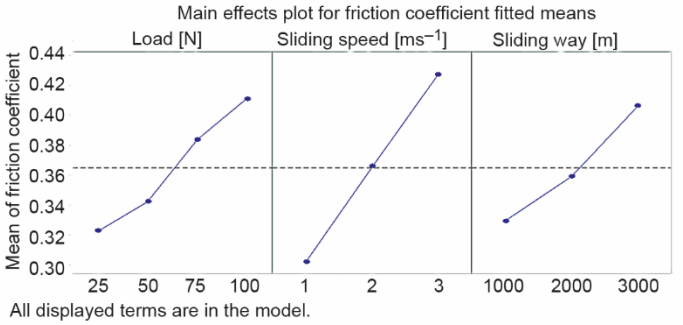

Figure 5. Average friction coefficient graphs for different loads, sliding speeds, and sliding ways

Temperature

Figure 6 shows the temperature interactions between materials for various loads, sliding speeds, and sliding ways. When the figure is examined, it is seen that the interaction values between the load-sliding way and sliding speed-sliding way are close. However, the interaction values between the load-sliding speed are high. This finding shows that the sliding speed is the most influential temperature parameter. As the sliding speed increases, the temperature between the materials increase.

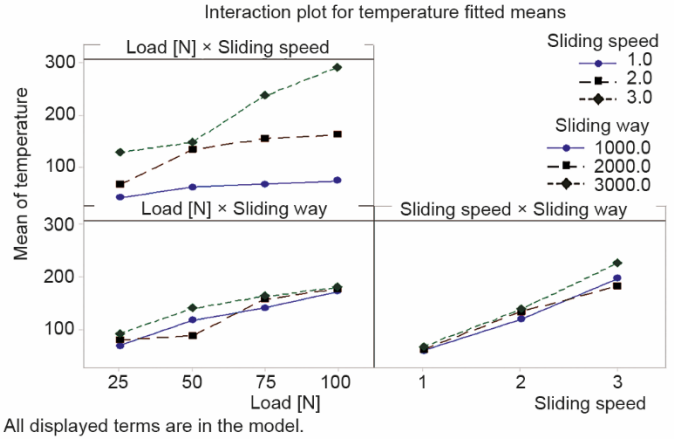

Figure 6. Temperature interaction graphs for various loads, sliding speeds, and sliding ways

An increase in the sliding speed causes an increase in temperature depending on the load. The maximum temperature value was obtained at a load of 100 N and a sliding speed of 3 m/s. The temperature value under these conditions is 299 °C. When the interaction of the load for the sliding speed is examined, the maximum temperature value was determined on a 100 N load and 3000 m sliding way. The minimum temperature value was determined on a 25 N load and 1000 m sliding way. When the temperature values were examined according to the interaction between the sliding speed and the sliding way, the minimum temperature value was obtained at 1 m/s sliding speed and 1000 m sliding way. As the contact material pressure and shear rate increase, the sample temperature and deformation rate increase. The rise in temperature is attributed to the increase in friction coefficient caused by the accumulation of particles on the disc due to wear. The literature states that the temperature proportionally increases with the friction coefficient and affects the wear mechanisms by forming oxidation between the materials [22-24].

Figure 7 shows the temperature changes between the materials and the minimum, maximum, and optimum temperature values for different loads, sliding speeds, and sliding ways. When the graph is examined, it is seen that all determined experimental parameters cause a temperature increase. It was determined that the most influential parameter was the sliding speed, the second most effective parameter was the load, and the least effective parameter was the sliding way. The highest temperature was recorded in the case of 100 N load, 3 m/s sliding speed, and 3000 m sliding way. The lowest temperature was recorded in the case of 25 N load, 1 m/s sliding speed, and 1000 m sliding way. The temperature in these optimum conditions giving the lowest value was measured as 37 ^{o}C.

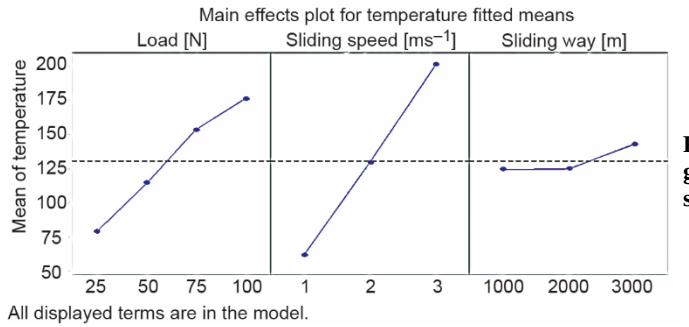

Figure 7. Average temperature graphs for various loads, sliding speeds, and sliding ways

Wear, friction coefficient, and temperature maps

The 3-D graphics showing the amount of wear in aluminum bronze alloys for different loads, sliding speeds, and sliding ways are shown in fig. 8. These graphs are wear maps created to understand and compare the effects of varying test parameters on weight loss in aluminum bronze alloys. When these figures are examined, it is understood that the parameters affecting the amount of wear are load, sliding speed, and sliding way, respectively. Maximum wear amount was determined at 100 N load, 3 m/s sliding speed, and 3000 m sliding way, while minimum wear amount was determined at 25 N load, 1 m/s sliding speed, and 1000 m sliding way. As the load and sliding speed increase, the sample's wear increases. Increasing amounts of wear cause permanent deformation and material losses in parts.

Figure 9 shows 3-D graphs showing the friction coefficient changes in aluminum bronze alloys for various loads, sliding speeds, and sliding ways. When the figure is examined, it is understood that the parameters affecting the friction coefficient are load, sliding speed, and sliding way, respectively. The maximum friction coefficient was determined for 100 N load, 3 m/s sliding speed, and 3000 m sliding way, while the minimum friction coefficient was determined for 25 N load, 1 m/s sliding speed, and 1000 m sliding way.

Figure 10 shows 3-D graphs showing the temperature changes between the aluminum bronze and the abrasive disc for various loads, sliding speeds, and sliding ways. The maximum temperature was determined for 100 N load, 3 m/s sliding speed, and 3000 m sliding way, while the minimum temperature value was determined at 25 N load, 1 m/s sliding speed, and 1000 m sliding way. It is seen that as the load and shear rate increase, the temperature and deformation of the sample increase. The rise in temperature and deformation rate increases wear particles' oxidation rate and strain hardening effect.

Wear mechanisms

The microstructures of aluminum bronze specimens tested at 100 N load, 1000 m sliding way, and 1 m/s, 2 m/s, and 3 m/s sliding speeds are given in fig. 11. When these images obtained by SEM are examined, surface roughness occurs at a sliding speed of 1 m/s, and local ruptures and separations occur as partial small particles. When the sliding speed reaches 2 m/s, larger spills and micro-cracks arise compared to the previous situation. When the sliding speed reaches 3 m/s, wavy surface morphology is formed on the spilled area surfaces, and therefore the surfaces begin to fatigue. When the SEM images are examined comparatively, it is understood that the sliding speed significantly affects the wear.

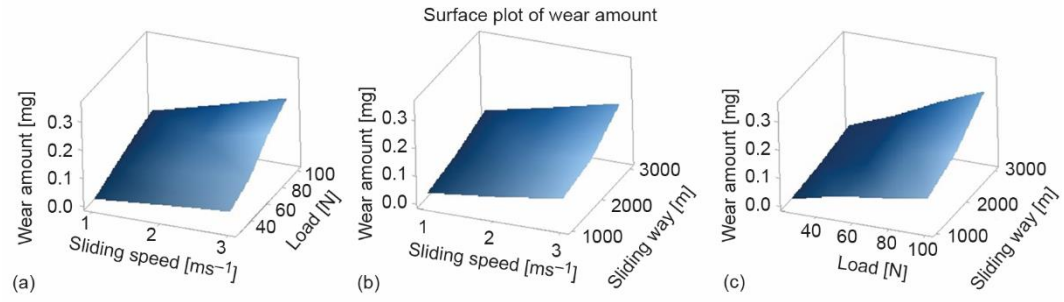

Figure 8. Surface plots of wear amount; (a) *vs.* load and sliding speed, (b) *vs.* sliding way and sliding speed, and (c) sliding way and load

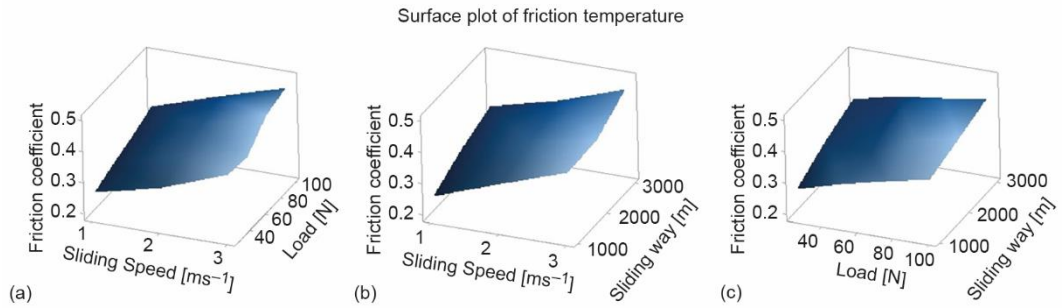

Figure 9. Surface plots of friction coefficient; (a) *vs.* load and sliding speed, (b) *vs.* sliding way and sliding speed, and (c) sliding way and load

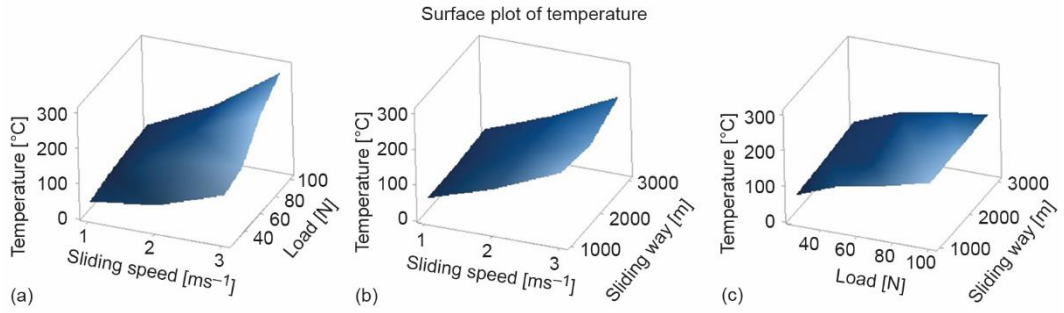

Figure 10. Surface plots of temperature; (a) *vs.* load and sliding speed, (b) *vs.* sliding way and sliding speed, and (c) sliding way and load

The SEM images of the wear occurring in the case of 100 N load, 2000 m sliding way, and 1 m/s, 2 m/s, and 3 m/s sliding speeds are shown in fig. 12. When the images are examined, it is seen that local ruptures and separations in larger sizes from the surfaces have started at 1 m/s speed compared to the 1000 m sliding way. Flattening and surface cracks occur on the surfaces at 2 m/s sliding speed. When the sliding speed rises to 3 m/s, wavy surface morphology and fatigue begin on the surfaces. Abrasive fatigue traces are visible in the images.

The SEM images showing wear traces at 100 N load, 3000 m sliding way, and 1 m/s, 2 m/s, and 3 m/s sliding speeds are shown in fig. 13. Local ruptures, flattening of surfaces, and local separations start at 1 m/s sliding speed. More shedding and fatigue cracks occur

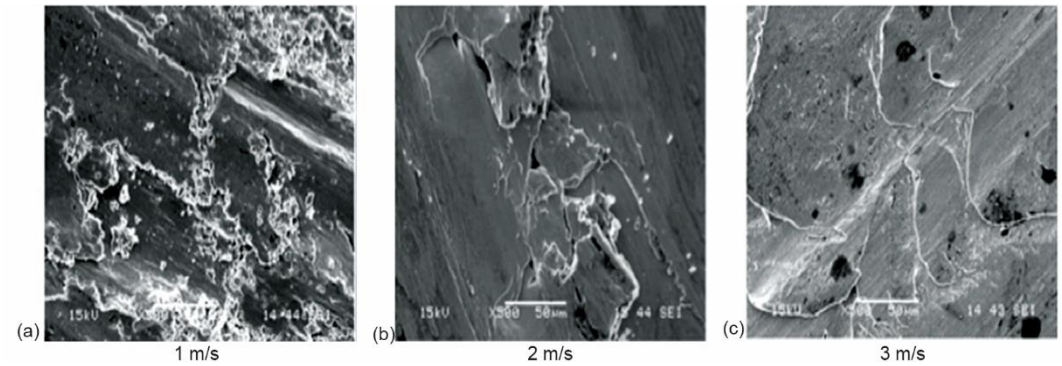

Figure 11. The SEM images at different sliding speeds for 100 N load and 1000 m sliding way

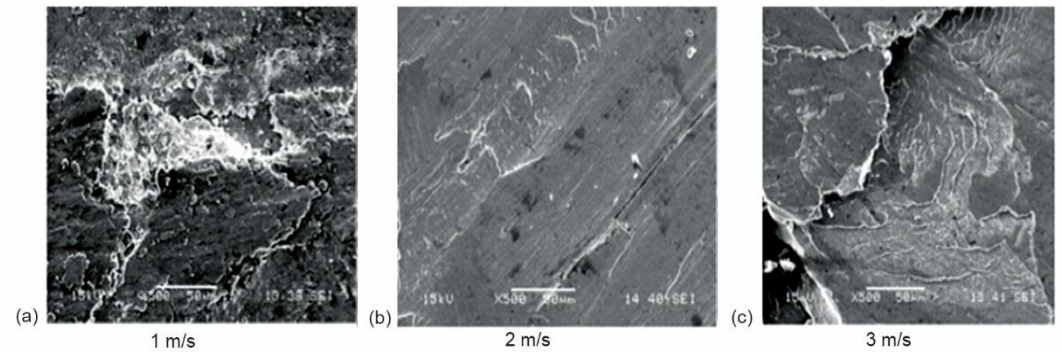

Figure 12. The SEM images at different sliding speeds for 100 N load and 2000 m sliding way

at a shear rate of 2 m/s. At a sliding speed of 3 m/s, wavy surface morphology and significant wear fatigue occur on the wear surface. Developing surface cracks cause the material layer to be separated and spilled on the surface, and a new surface emerges.

Maximum wear occurs at different sliding way values at 100 N load and 3 m/s. When these wear surfaces are compared, it is observed that the wear fatigue marks increase significantly after 2000 m, and a new surface continues to wear fatigue from the bottom with the separation of the wear layer from the surface. It is understood from the SEM images that the sliding way is also an effective parameter of the wear mechanisms.

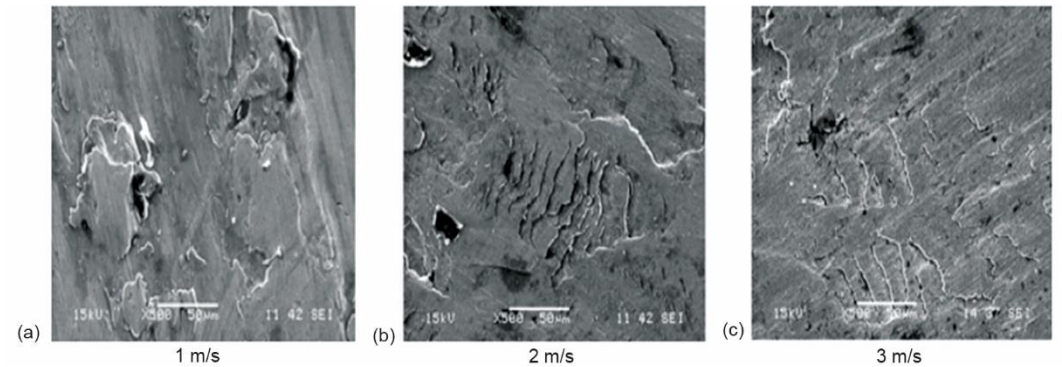

Figure 13. The SEM images at different sliding speeds for 100 N load and 3000 m sliding way

Conclusions

This study analyzed the tribological features of aluminum bronze alloy samples created through the forging process. The AISI8620 cementation steel was used as the abrasive material by hardening. The loads applied in the experiments were 25 N, 50 N, 75 N, and 100 N, sliding speeds of 1 m/s, 2 m/s, and 3 m/s, and sliding ways of 1000 m, 2000 m, and 3000 m.

With the increased applied load, the weight losses in the sample increased linearly. The maximum wear amount was under 100 N load, and the minimum was under 25 N load. The wear losses of the specimens increased linearly with the increase in the sliding speed. The highest weight loss occurred at the sliding speed of 3 m/s. A load of 100 N, a sliding speed of 3 m/s, and a wear amount of 3000 m sliding way is 0.352 mg. With the sliding way increase, the weight losses of the samples also increased linearly. The increase in load, sliding speed, and sliding way cause an increase in the friction coefficient. The minimum coefficient of friction was determined in the case of 25 N load, 1 m/s sliding speed, and 1000 m sliding way, while the maximum friction coefficient was determined in the case of 100 N load, 3 m/s sliding speed, and 3000 m sliding way. The increase in load, sliding speed, and sliding way also causes an increase in temperature in the samples. The lowest temperature on the wearing surfaces is 37 °C, and the highest is 299 °C. When the microstructure images are examined, it is seen that there are local ruptures in the materials, flattening on the surfaces, increases in the surface roughness, local shedding, and wear fatigue, depending on the sliding speed.

As a result of experimental studies, it is understood that applied load, sliding speed, and sliding way are effective parameters in wear, friction coefficient, and temperature changes. If these parameters are reduced, material losses, abrasions, and deformations in the parts will decrease, and the life of the parts will be extended.

References

[1] Shajari, Y., *et al.*, Improvement of the NiBrAl Casting Alloy Surface Properties by Electroless Ni-B Plating for Dynamic Marine Applications, *Phys. Mesomech., 23* (2020), 1, pp. 81-88
[2] Heidarzadeh, A., *et al.*, Friction Stir Welding/Processing of Metals and Alloys: A Comprehensive Review on Microstructural Evolution, *Prog. Mater. Sci., 117* (2021), Apr., 100752
[3] Kear, G., *et al.*, Flow Influenced Electrochemical Corrosion of Nickel Aluminium Bronze – Part I. Cathodic Polarisation, *J. Appl. Electrochem., 34* (2004), 12, pp. 1235-1240
[4] Luo, Q., *et al.*, The Synergistic Effect of Cavitation Erosion and Corrosion of Nickel-Aluminum Copper Surface Layer on Nickel-Aluminum Bronze Alloy, *J. Alloys Compd., 747* (2018), May, pp. 861-868
[5] Asghar, A., *et al.*, Nickel-Aluminium Bronze (NiBRAl) Casting Alloy Tribological/Corrosion Resistance Properties Improvement *via* Deposition of a Cu-Doped Diamond-Like Carbon (DLC) thin Film ; Optimization of Sputtering Magnetron Process Conditions, *Mater. Chem. Phys., 296* (2023), Feb., 127279
[6] Shen, C., *et al.*, The Influence of Post-Production Heat Treatment on the Multi-Directional Properties of Nickel-Aluminum Bronze Alloy Fabricated Using Wire-Arc Additive Manufacturing Process, *Addit. Manuf., 23* (2018), Oct., pp. 411-421
[7] Yang, F., *et al.*, The Role of Nickel in Mechanical Performance and Corrosion Behaviour of Nickel-Aluminium Bronze in 3.5 wt.% NaCl Solution, *Corros. Sci., 139* (2018), July, pp. 333-345
[8] Yang, F., *et al.*, Electrochemical Corrosion Mechanisms of Nickel-Aluminium Bronze with Different Nickel Contents Using the Rotating Disc Electrode, *Corros. Sci., 157* (2019), Aug., pp. 438-449
[9] Hazra, M., Balan, K. P., Failure of a Nickel Aluminium Bronze (NAB) Canned Motor Pump Impeller Working Under Polluted Sea Water – Influence of Material Selection, Section Thickness Dependent Microstructure and Temper Annealing Heat Treatment, *Eng. Fail. Anal., 70* (2016), Dec., pp. 141-156
[10] Zhang, B., *et al.*, Load-Dependent Tribocorrosion Behaviour of Nickel-Aluminium Bronze in Artificial Seawater, *Corros. Sci., 131* (2018), Feb., pp. 252-263

[11] Rahni, B., *et al.*, Effect of Filler Metal on Microstructure and Mechanical Properties of Manganese-Aluminum Bronze Repair Welds, *Trans. Nonferrous Met. Soc. China*, *27* (2017), 3, pp. 507-513
[12] Demircioglu, P., Topological Evaluation of Surfaces in Relation to Surface Finish, *Comprehensive Materials Finishing*, *3* (2017), 17, pp. 243-260
[13] Bogrekci, I., Demircioglu, P., Evaluation of Surface Finish Quality Using Computer Vision Techniques, *Comprehensive Materials Finishing*, *3* (2017), 18, pp. 261-275
[14] Tan, K. S., *et al.*, Solid Particle Erosion-Corrosion Behaviour of a Novel HVOF Nickel Aluminium Bronze Coating for Marine Applications – Correlation Between Mass Loss and Electrochemical Measurements, *Wear*, *258* (2005), 1-4, pp. 629-640
[15] Liu, X., *et al.*, Multi-Directional Forging and Aging Treatment Effects on Friction and Wear Characterization of Aluminium-Bronze Alloy, *Mater. Charact.*, *167* (2020), Sept., 11051
[16] Kucita, P., *et al.*, The Effects of Substrate Dilution on the Microstructure and Wear Resistance of PTA Cu-Al-Fe Aluminium Bronze Coatings, *Wear*, *440* (2019), Dec., 203102
[17] Gamon, W., Aniolek, K., Examination of the Sliding Wear of Bronze Coatings on Railway Buffer Heads, *Wear*, *448* (2020), May, 203235
[18] Kirubakaran, J., *et al.*, Wear Behavior Analysis of Aluminium Composites Using Taguchi Approach, *Mater. Today Proc.*, *64* (2022), 1, pp. 345-351
[19] Gurav, P., *et al.*, Optimizing Tribological Performance of Laser-Induced Elliptical Textures on Nickel Aluminum Bronze Surface based on Genetic Algorithm, *J. Mater. Eng. Perform.*, *32* (2023), Sept., pp. 4676-4690
[20] Thapliyal, S., Dwivedi, D. K., Study of the Effect of Friction Stir Processing of the Sliding Wear Behavior of Cast NiAl Bronze: A Statistical Analysis, *Tribol. Int.*, *97*(2016), May, pp. 124-135
[21] Sımsek, D., *et al.*, Dry Sliding Wear Behaviors of Iron Addition to Nickel-Aluminum Bronze Produced by Mechanical Alloying, *Trans. Indian Inst. Met.*, *73* (2020), 2, pp. 319-326
[22] Yaşar, M., Altunpak, Y., The Effect of Aging Heat Treatment on the Sliding Wear Behaviour of Cu-Al-Fe Alloys, *Mater. Des.*, *30* (2009), 3, pp. 878-884
[23] Li, Y., *et al.*, Mechanical, Friction and Wear Behaviors of a Novel High-Strength Wear-Resisting Aluminum Bronze, *Wear*, *197* (1996), 1-2, pp. 130-136
[24] Kimura, T., *et al.*, Sliding Wear Characteristic Evaluation of Copper Alloy for Bearing, *Wear*, *263* (2007), 1-6, pp. 586-591

Paper submitted: September 25, 2022
Paper revised: March 12, 2023
Paper accepted: May 15, 2023

© 2023 Society of Thermal Engineers of Serbia.
Published by the Vinča Institute of Nuclear Sciences, Belgrade, Serbia.
This is an open access article distributed under the CC BY-NC-ND 4.0 terms and conditions.